

Cosmic reverberations on a constrained $f(Q, T)$ -model of the Universe

Akanksha Singh,^{1,*} Shaily,^{1,2,†} and J. K. Singh^{1,‡}

¹*Department of Mathematics, Netaji Subhas University of Technology, New Delhi-110 078, India*

²*School of Computer Science Engineering and Technology, Bennett University, Greater Noida, India*

In this paper, we construct an isotropic cosmological model in the $f(Q, T)$ theory of gravity in the frame of a flat FLRW spacetime being Q the non-metricity tensor and T the trace of the energy-momentum tensor. The gravity function is taken to be a quadratic equation, $f(Q, T) = \zeta Q^2 + \gamma T$, where $\zeta < 0$ and γ are the arbitrary constants. We constrain the model parameters α and H_0 using the recent observational datasets: the Hubble dataset (OHD), the Pantheon dataset of 1048 points, and the joint dataset (OHD + Pantheon). The universe model transits from an early deceleration state to an acceleration in late times. This model also provides the ekpyrotic phase of the universe on the high redshift $z > 12.32$. In this model, the Big Bang is described as a collision of branes, and thus, the Big Bang is not the beginning of time. Before the Big Bang, there is an ekpyrotic phase with the equation of state $\omega \gg 1$. In late times, the undeviating Hubble measurements reduce the H_0 tension in the reconstructed $f(Q, T)$ function. Additionally, we study various physical parameters of the model. Finally, our model describes a quintessence dark energy model at later times.

PACS numbers: 98.80 Cq.

Keywords: $f(Q, T)$ -gravity, observational analysis, ekpyrotic phase, quintessence model, scalar field, slow-roll parameters.

I. INTRODUCTION

The human accomplishment to observe more clearly has led to the discovery of differences between theoretical models and empirical evidence these days. It is believed that the cosmos is in its expansion phase, and it is interesting to note that the universe had a fast expansion just after the Big Bang, referred to as the inflationary era. The literature has examined various directions to understand the phase-transition behavior from early-time deceleration to late-time acceleration. In the last three decades, cosmologists have made some surprising observations that have concluded that the expansion nature of the universe is behaving in an accelerating manner [1–7]. Such observations completely changed the thinking of cosmologists, who then reviewed Einstein’s theory, which contains the cosmological constant. This accelerating expansion of the universe indicates the presence of dark sectors. Until now, various cosmological models have been proposed that try to mock up this era with others using different approaches like scalar fields, modified gravity in distinct forms, etc.

When we deal with the theory of gravitation, there are many existing potential theories in which General Relativity (GR) is the foundation of these various conceivable nonlinear gravity theories (NLG). Modified theories of gravity are nothing but some modifications, generalizations, and complications of Einstein’s GR. However, these modified theories are not able to fully explain the mysterious questions. The theory of GR is indeed a milestone achievement for us. Some concepts of GR have given a new direction to describing the universe. Several observational phenomena like black holes, neutron stars, and gravitational waves were determined during the 20th century. Although GR is highly tested, the door for alternatives to GR is always open. According to the probes, the behavior of 95% of the universe’s matter content is unknown. GR is not enough to describe gravity completely as it does not engage the local energy-momentum tensor (EMT) [8–10]. This theory is not able to explain the reason for speeding up the expansion of the universe and is also inadequate to describe the most curious energy, i.e., dark energy, which covers around 70% of the universe. Therefore, in the last few decades, modified theories of gravity have become more famous because of better explanations regarding dark energy, dark matter, the expanding nature of the universe, etc. The modified theory of gravity discusses the early universe and the late-time universe. The phase transition from early-time deceleration to late-time acceleration, along with variation from the non-phantom phase to the phantom phase without involving exotic matter.

Many of the excellent works have been done in the field of modified theories of gravity, including the scale-independent theory of Weyl, Eddington’s theory of connections [11], the scalar-tensor theory [12–15], string theory [16–18], Brans-Dicke’s theory [19–22], the higher-dimensional theory of Kaluza-Klein, $f(R, T)$ gravity [23–35], $f(R, G)$

* akanksha.ma19@nsut.ac.in

† shailytyagi.iitkgp@gmail.com

‡ jksingh@nsut.ac.in

gravity [36–39], $f(R, L_m)$ gravity [40, 41], $f(Q, C)$ gravity [42], and other so many works have been done in modified theories of gravity [43–54, 62–64]. Jean-Luc Lehnars studied the ekpyrotic and cyclic phases of the universe, which provides the theory of the very early and very late universes. In these models, the Big Bang is described as a collision of branes and thus the Big Bang is not the beginning of time. Before the big bang, there was an ekpyrotic phase with the equation of state $\omega \geq 1$ during which the universe slowly contracts [65].

Recently, the study of modified theories of gravity has focused on $f(Q, T)$ gravity. The $f(Q, T)$ gravity is an extension of $f(Q)$ gravity that is developed with the help of the symmetric teleparallel equivalent of GR. In $f(Q)$ gravity, curvature, and torsion vanish, leaving just the non-metricity tensor Q to describe the gravitational interaction. Several different properties for this gravity have been discussed [66–77]. The gravity theory $f(Q, T)$, that combines the effects of the non-metricity tensor and the trace of the EMT, has been the subject of several studies [78–91]. The historical development of gravitational theories leading up to $f(Q, T)$ gravity has been marked by significant advancements. Harko and Lobo [43] expanded on the development of modified theories of gravity, including those with generalized curvature-matter couplings and hybrid metric-Palatini gravity, setting the stage for the emergence of $f(Q, T)$ gravity. Golovnev and Guzmán [47] discussed foundational issues in $f(T)$ gravity theory, which shares similarities with $f(Q, T)$ gravity and provides valuable insights into the theoretical underpinnings of these modified gravitational theories. There is a sub-classification of $f(Q, T)$ gravity known as Weyl type $f(Q, T)$ gravity in which the function $f(Q, T)$ is selected to adhere to specific properties consistent with the Weyl geometry [83–85].

The concept of $f(Q, T)$ gravity, an extension of symmetric teleparallel gravity, has significant implications in theoretical physics and various astrophysical and cosmological contexts. It introduces a function f of the non-metricity tensor Q and the trace of the matter EMT T , leading to non-conservation of energy-momentum and accelerating expansion of the universe [86, 88]. This theory has been applied to various cosmological models with and without dark energy or dark matter and has been found to obey energy conditions and support the accelerating behavior of the universe [77, 91]. These findings suggest that $f(Q, T)$ gravity has the potential to reshape our understanding of gravity and its manifestations in cosmology. Cai et al. [48] and Kofinas, along with Saridakis [51] both explore its cosmological applications, with Cai focusing on the late-time universe acceleration and Kofinas on the unified description of cosmological history. Heisenberg [77] highlights its potential to provide new insights into the nature of gravity, address computational and conceptual questions, and reshape our understanding of gravity in cosmology. This paper also further discusses its potential in early and late-time cosmology, black holes, and wormholes, without the need for dark energy, inflaton fields, or dark matter. These studies collectively demonstrate the versatility and potential of $f(Q, T)$ gravity in advancing our understanding of the universe. Godani and Samanta [89] further investigate its application in the Friedmann-Robertson-Walker (FRW) model, using Hubble and Supernova data to constrain model parameters and compare results with the Λ CDM model. The development of cosmological perturbation theory in $f(Q, T)$ gravity has provided a framework for testing these models with observational data, potentially shedding light on the Hubble constant tension and the nature of dark matter [90].

The content of the work is organized as follows: Sect. II contains an overview of the $f(Q, T)$ theory, the process for finding the field equations using the Einstein-Hilbert action of $f(Q, T)$ gravity, and evaluating various physical parameters. In Sect. III, we find the best-fit values of the model parameters using the Hubble datasets of 77 points, the *Pantheon* datasets of 1048 points, and their joint datasets to constrain all the model parameters. In Sect. IV, we analyze the behavior of the various cosmological parameters using the constrained model parameters. The analysis of the energy conditions, the scalar field, and the slow-roll parameters have been performed in the various subsections of the Sect. IV. Finally, we interpret the physical results of the model in Sect. V.

II. THE $f(Q, T)$ -GRAVITY AND THE EINSTEIN FIELD EQUATIONS

The Einstein-Hilbert action for the modified gravity theory $f(Q, T)$ is [86]

$$S = \int \left[\frac{1}{16\pi} f(Q, T) + S_m \right] \sqrt{-g} d^4x, \quad (1)$$

where $f(Q, T)$ is any function depends Q and T . The notation S_m is for the Lagrangian of a given matter. The quantity Q is given by

$$Q \equiv -g^{\mu\nu} (L^\alpha_{\beta\mu} L^\beta_{\nu\alpha} - L^\alpha_{\beta\alpha} L^\beta_{\mu\nu}), \quad (2)$$

where $L^\alpha_{\beta\gamma}$, the disformation tensor can be calculated by the definition

$$L^\alpha_{\beta\gamma} \equiv -\frac{1}{2} g^{\alpha\lambda} (\nabla_\gamma g_{\beta\lambda} + \nabla_\beta g_{\lambda\gamma} - \nabla_\lambda g_{\beta\lambda}). \quad (3)$$

The variation of the action represented by Eq. (1) gives the field equations obtained as

$$-\frac{2}{\sqrt{-g}}\nabla_{\alpha}(f_Q\sqrt{-g}P^{\alpha}_{\mu\nu})-\frac{1}{2}fg_{\mu\nu}+f_T(T_{\mu\nu}+\Theta_{\mu\nu})-f_Q(P_{\mu\alpha\beta}Q_{\nu}^{\alpha\beta}-2Q^{\alpha\beta}_{\nu}P_{\alpha\beta\nu})=8\pi T_{\mu\nu}. \quad (4)$$

Here, $f_Q = \frac{\partial f}{\partial Q}$, $f_T = \frac{\partial f}{\partial T}$, and $P^{\alpha}_{\mu\nu}$ is the superpotential of the model [86]. The terms energy-momentum tensor ($T_{\mu\nu}$) and $\Theta_{\mu\nu}$ are written as

$$T_{\mu\nu} \equiv -\frac{2}{\sqrt{-g}}\frac{\delta(\sqrt{-g}S_m)}{\delta g^{\mu\nu}} \quad (5)$$

and

$$\Theta_{\mu\nu} \equiv g^{\alpha\beta}\frac{\delta T_{\alpha\beta}}{\delta g^{\mu\nu}}. \quad (6)$$

The flat, isotropic, and homogeneous FLRW line element is stated as

$$ds^2 = -dt^2 + a^2(t)(dx^2 + dy^2 + dz^2), \quad (7)$$

being $a(t)$ the scale factor.

We consider a non-metricity scalar $Q = 6H^2$. and the energy-momentum tensor for the perfect fluid-filled universe is assumed as:

$$T_{\nu}^{\mu} = \text{diag}(-\rho, p, p, p), \quad (8)$$

where ρ and p are the energy density and isotropic pressure of the universe, respectively. Using Eq. (8), $T = -\rho + 3p$. The expression for the tensor Θ_{ν}^{μ} is given by

$$\Theta_{\nu}^{\mu} = \text{diag}(2\rho + p, -p, -p, -p). \quad (9)$$

Using Eqs. (4), (5), (6), and (7), the generalized Friedmann equations can be determined as

$$8\pi\rho = \frac{f}{2} - 6FH^2 - \frac{2\tilde{G}}{1+\tilde{G}}(\dot{F}H + F\dot{H}), \quad (10)$$

$$8\pi p = -\frac{f}{2} + 6FH^2 + 2(\dot{F}H + F\dot{H}), \quad (11)$$

where $F \equiv f_Q$, $8\pi\tilde{G} \equiv f_T$, and the overhead dot represents the differentiation of that respective function concerning time t . We take the function $f(Q, T) = \zeta Q^2 + \gamma T$, $\zeta < 0$, which is motivated by some distinct research works [86, 87].

Using Eqs. (10), (11) and $f(Q, T)$, the field equations yield

$$8\pi\rho = \frac{1}{2}(\zeta Q^2 + \gamma T) - 12\zeta QH^2 - \frac{2\gamma}{8\pi + \gamma}(24\zeta H^2\dot{H} + 2\zeta Q\dot{H}), \quad (12)$$

$$8\pi p = -\frac{1}{2}(\zeta Q^2 + \gamma T) + 12\zeta QH^2 + 2(24\zeta H^2\dot{H} + 2\zeta Q\dot{H}). \quad (13)$$

Now, taking $Q = 6H^2$ and $T = -\rho + 3p$, the field equations (12), (13) reduce to

$$\left(\frac{16\pi + \gamma}{2}\right)\rho = \frac{3\gamma}{2}p - 54\zeta H^4 - \frac{72\gamma\zeta}{8\pi + \gamma}H^2\dot{H}, \quad (14)$$

$$\left(\frac{16\pi + 3\gamma}{2}\right)p = \frac{\gamma}{2}\rho + 54\zeta H^4 + 72\zeta H^2\dot{H}. \quad (15)$$

Solving Eqs. (14) and (15), we get the energy density ρ and isotropic pressure p as

$$\rho = \frac{9\zeta H^2 \left(-3(8\pi + \gamma)H^2 + 2\gamma\dot{H} \right)}{(4\pi + \gamma)(8\pi + \gamma)}, \quad (16)$$

and

$$p = \frac{9\zeta H^2 \left(3(8\pi + \gamma)H^2 + 2(16\pi + 3\gamma)\dot{H} \right)}{(4\pi + \gamma)(8\pi + \gamma)}. \quad (17)$$

we consider the jerk parameter j as a function of the redshift z , and is given by

$$j(z) = q(z) + 2q(z)^2 + (1+z) \frac{dq(z)}{dz}. \quad (18)$$

Eq. (18) contains two unknown parameters $j(z)$ and $q(z)$. So, we assume one of these two parameters to evaluate the other. Some of the researchers parametrized the jerk parameter to construct their cosmological models [92, 93]. Similarly, we consider $j(z) = e^{q(z)}$ and tried to solve the differential equation (18). To reduce the intricacy of the calculations, we take the first three terms of Maclaurin's expansion of $e^{q(z)}$ as $j(z) = 1 + q(z) + \frac{q^2(z)}{2}$.

Now, putting $j(z) = 1 + q(z) + \frac{q^2(z)}{2}$ in Eq. (18) and solving, we get

$$q(z) = -\frac{\sqrt{2/3} \left(e^{2\sqrt{6}\alpha} - (1+z)^{\sqrt{6}} \right)}{e^{2\sqrt{6}\alpha} + (1+z)^{\sqrt{6}}}, \quad (19)$$

where α is an arbitrary integration constant.

The deceleration parameter q in terms of the Hubble parameter H and redshift z is

$$q(z) = -1 + \frac{(1+z)}{H(z)} \frac{dH}{dz}. \quad (20)$$

Using Eqs. (19) and (20), the Hubble parameter $H(z)$ is given by

$$H(z) = \beta (1+z)^{1-\sqrt{2/3}} \left(e^{2\sqrt{6}\alpha} + (1+z)^{\sqrt{6}} \right)^{2/3}, \quad (21)$$

where β is an arbitrary integration constant.

Here, we define β as $\frac{H_0}{(e^{2\sqrt{6}\alpha} + 1)^{2/3}}$, where H_0 is the present value of the Hubble parameter $H(z)$, and Eq. (21) reduce to

$$H(z) = \frac{H_0}{(e^{2\sqrt{6}\alpha} + 1)^{2/3}} (1+z)^{1-\sqrt{2/3}} \left(e^{2\sqrt{6}\alpha} + (1+z)^{\sqrt{6}} \right)^{2/3}. \quad (22)$$

III. THE STATISTICAL ANALYSIS OF THE MODEL

To estimate the observational constraints of the model parameters, we use different datasets employed in this work and deliberate about the methodology used to constrain the free parameters. The Markov Chain Monte Carlo (MCMC) sampling technique optimizes the values of model parameters in Python coding with the EMCEE library. We employ the newly published $H(z)$ dataset and the *Pantheon* dataset in Python coding. The $H(z)$ dataset contains 77 observations of cosmic chronometers that span a redshift range $0 \leq z \leq 2.36$. The *Pantheon* dataset comprises 1048 observations of Supernova Type Ia that span a redshift range $0.01 \leq z \leq 2.26$. The *Pantheon* datasets have been collected from various surveys, namely, high- z , PS1, SDSS, SNLS, low- z , HST, CfA 1-4, etc. (refer to Table I) [94].

TABLE I: The *Pantheon* datasets survey.

Surveys	The data points	Redshift range	References
CfA 1-4	147	0.01 – 0.07	[95–99]
CSP	25	0.01 – 0.06	[100]
SDSS	335	0.03 – 0.40	[101]
SNLS	236	0.12 – 1.06	[102]
PS1	279	0.02 – 0.63	[103]
high- z	26	0.73 – 2.26	[104–107]
Total	1048	0.01 – 2.26	

It is noted that $H(z) = -\frac{1}{1+z} \frac{dz}{dt}$. Using the $H(z)$ dataset we calculate the best-fit values of model parameters α and H_0 by minimizing the value of χ^2 . The formula for minimizing χ^2 is given by

$$\chi_{HDS}^2(\alpha, H_0) = \sum_{i=1}^{77} \left[\frac{H_{th}(\alpha, H_0, z_i) - H_{ob}(z_i)}{\sigma_{H(z_i)}} \right]^2, \quad (23)$$

where χ_{HDS}^2 represents the value of χ^2 for the Hubble dataset, $H(z_i)$ is obtained at redshift z_i , and H_{th} and H_{ob} indicate the theoretical and observed values of Hubble parameter, respectively. The standard error in H_{ob} is indicated by $\sigma_{H(z_i)}$.

The *Pantheon* data collected through various surveys plays a prominent role in investigating the expanding nature of the universe. Using the theoretically estimated apparent magnitude (m) and absolute magnitude (\mathcal{M}) in regards to the color and the stretch, we determine the value of the distance modulus $\mu_{th}(z_i)$ as

$$\mu(z) = m - \mathcal{M} = 5 \text{Log} \mathcal{D}_L(z) + \mu_0. \quad (24)$$

For the flat universe, the luminosity distance $\mathcal{D}_L(z) = (1+z)c\mathcal{D}_m \int_0^z \frac{1}{H(w)} dw$, where $\mathcal{D}_m(z)$ is defined as

$$\mathcal{D}_m(z) = \begin{cases} \frac{\sinh(\sqrt{\Omega_n})}{H_0 \sqrt{\Omega_n}}, & \text{for } \Omega_n > 0 \\ 1, & \text{for } \Omega_n = 0 \\ \frac{\sin(\sqrt{\Omega_n})}{H_0 \sqrt{\Omega_n}}, & \text{for } \Omega_n < 0 \end{cases} \quad (25)$$

and the nuisance parameter μ_0 is given as

$$\mu_0 = 5 \text{Log} \left(\frac{H_0^{-1}}{1 \text{Mpc}} \right) + 25. \quad (26)$$

The maximum likelihood method is used to constrain the values of α and H_0 . The relevant χ^2 function is given by

$$\chi_{PDS}^2(\alpha, H_0) = \sum_{i=1}^{1048} \left[\frac{\mu_{th}(\alpha, H_0, z_i) - \mu_{obs}(z_i)}{\sigma_{\mu(z_i)}} \right]^2, \quad (27)$$

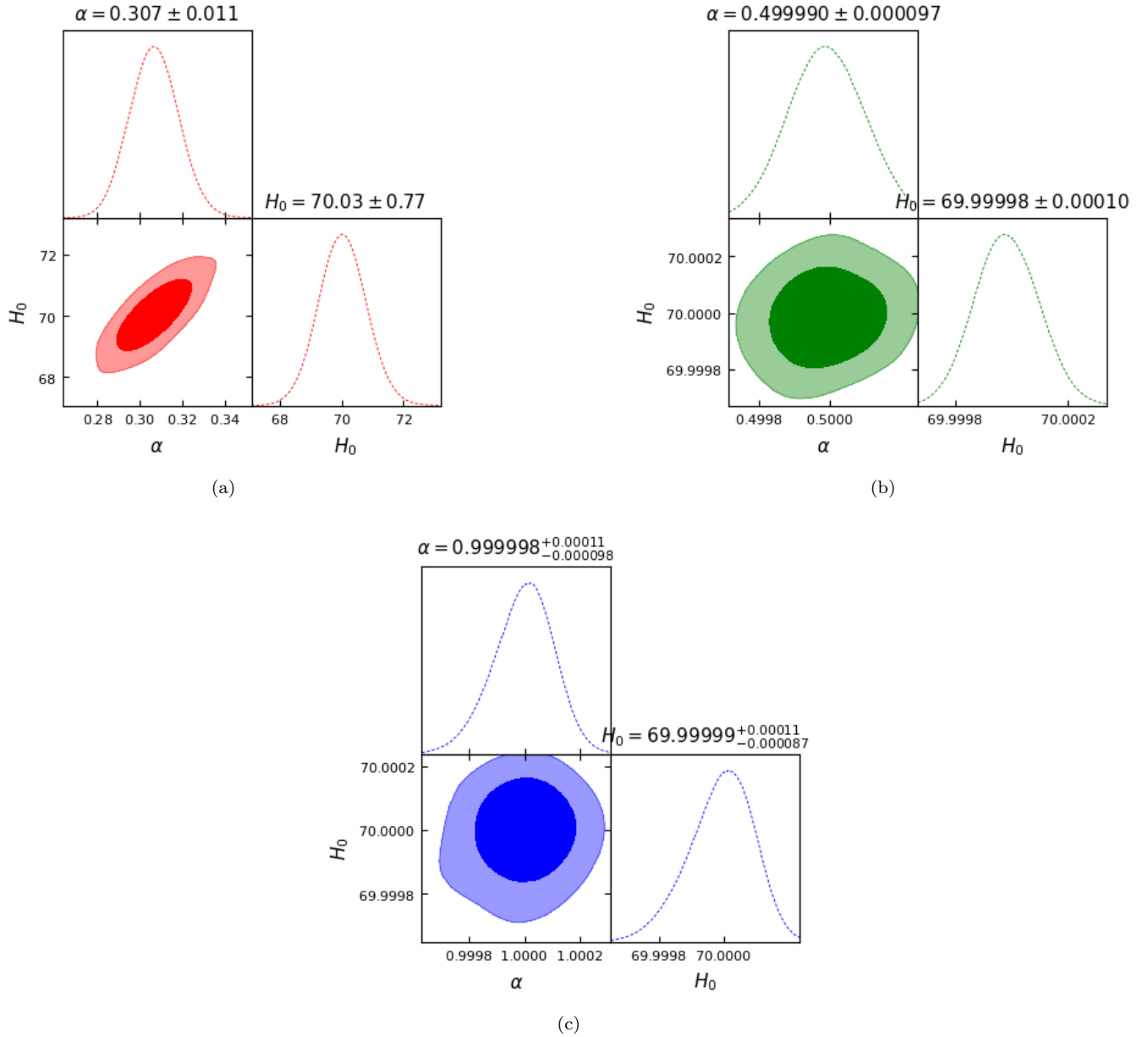


FIG. 1: The posterior distribution of the $f(Q, T)$ model for 1 σ and 2 σ CLs obtained from the OHD, Pantheon, and OHD+Pantheon datasets respectively.

where PDS represents the observational *Pantheon* dataset. μ_{th} and μ_{obs} are used for the theoretical and observed distance moduli of this model, respectively, and $\sigma_\mu(z_i)$ indicates the standard error in the observed value.

We employ joint statistical analysis by using both datasets, i.e., Hubble samples and *Pantheon* samples. This joint analysis gives better constraints. For this purpose, the χ^2 function is specified as

$$\chi^2_{Joint} = \chi^2_{OHD} + \chi^2_{PDS}. \quad (28)$$

For all three datasets, the constrained values of the model parameters have been summarized in Table II.

TABLE II: The constrained values of the model parameters.

Dataset	α	H_0	z_{tr}^a	q_0^b	p_{tr}^{cd}
OHD	0.307 ± 0.011	70.03 ± 0.77	0.84781	-0.519567	0.47
Pantheon	0.49999 ± 0.000097	69.99998 ± 0.0001	1.71823	-0.686707	1.14
H(z)+Pantheon	$0.99999^{+0.00011}_{-0.000098}$	$69.99999^{+0.00011}_{-0.000087}$	6.38903	-0.804414	4.79

^a Transitions from deceleration to acceleration

^b The present value of the q

^c Transitions of isotropic pressure from positive to negative

^d $\lim_{z \rightarrow -1} p = 0$

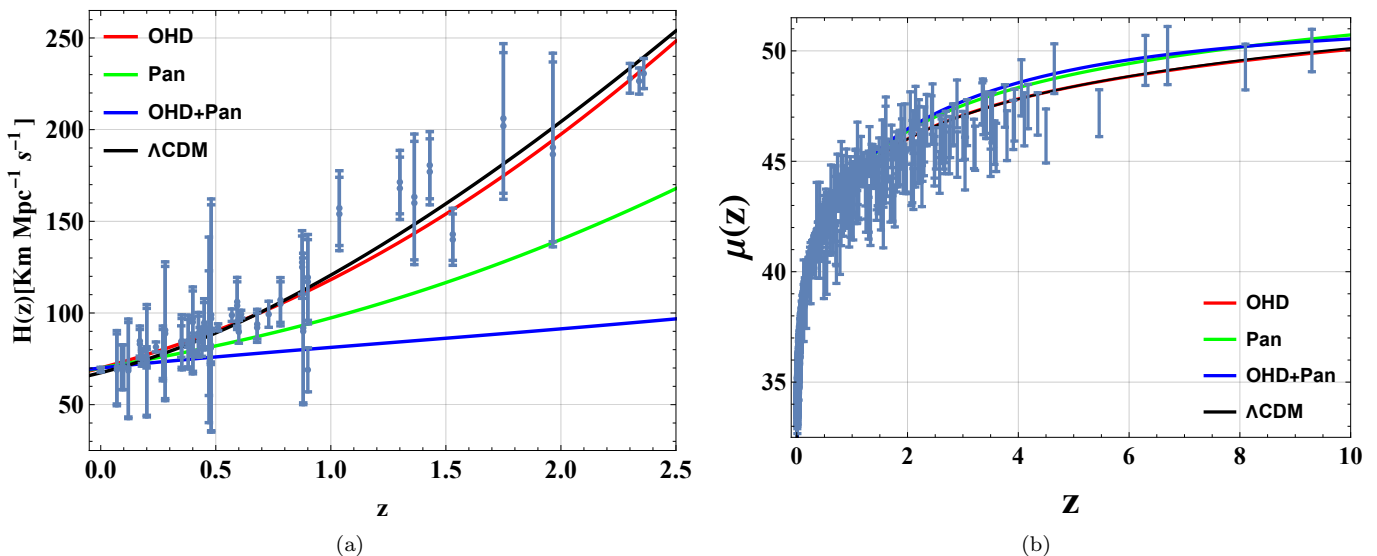


FIG. 2: The likeness of our model with ΛCDM for OHD, Pantheon, OHD + Pantheon datasets in the Error Bar plots.

IV. THE COSMOLOGICAL PARAMETERS

In this section, we discuss the physical behaviors of the model. With the help of the scale factor's first-order derivative and higher derivative components, we can analyze the geometrical and dynamic nature of the cosmos more competently. The Hubble parameter H , the deceleration parameter q , and the jerk parameter j can be expressed as $H = \frac{\dot{a}}{a}$, $q = -\frac{\ddot{a}a}{\dot{a}^2}$, $j = \frac{\ddot{\dot{a}}a^2}{\dot{a}^3}$.

We analyze the evolution of these cosmic parameters using different plots according to the constraints on α and H_0 mentioned in Table II. In Fig. 2a, one can notice that H decreases monotonically as $z \rightarrow -1$, which shows that the expansion rate is high at the early stage of evolution, and decreases in later times. The dimensionless deceleration parameter q exhibits the transition from early deceleration to acceleration at later times (see Fig. 3a). The transitional redshifts (z_{tr}) are 0.847808, 1.71823, and 6.38903, and q_0 are -0.519567, -0.686707, and -0.804414 for different observations shown in Table II. Using Eq. (19) in the expression $1 + q(z) + \frac{q^2(z)}{2}$, the jerk parameter j

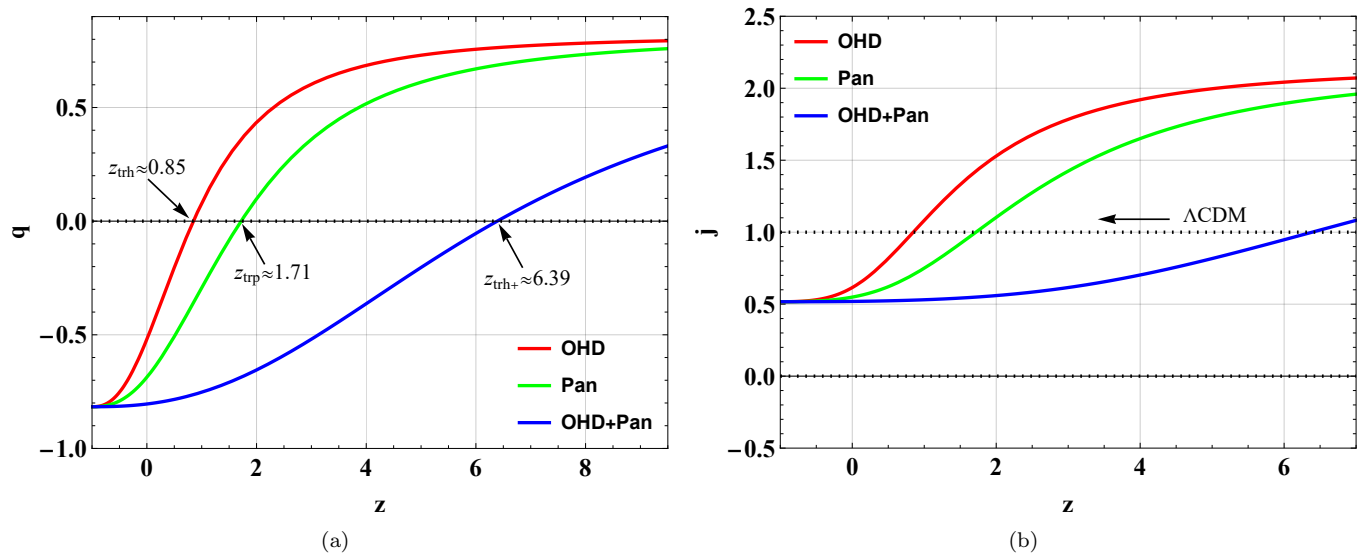


FIG. 3: The evolution of q and j .

can be calculated as

$$j = \frac{(4 - \sqrt{6}) e^{4\sqrt{6}\alpha} + 4e^{2\sqrt{6}\alpha} (z+1)^{\sqrt{6}} + (4 + \sqrt{6}) (z+1)^{2\sqrt{6}}}{3 \left(e^{2\sqrt{6}\alpha} + (z+1)^{\sqrt{6}} \right)^2}. \quad (29)$$

In Fig. 3b, the jerk parameter j is different from 1 for each dataset, which indicates that our obtained model deviates from the Λ CDM defined by $j = 1$.

Using the expression $\dot{H} = -(1+z)H(z)\frac{dH}{dz}$ and Eq. (22) in Eqs. (16) and (17), we evaluate ρ and p as the functions of z . The trajectories in Figs. 4a and 4b depict that ρ and p decrease monotonically during the evolution for OHD, *Pantheon*, and OHD+*Pantheon* datasets. In Fig. 4b, p transits from a positive to a negative value in the redshift range $0.47 \leq z \leq 4.79$ which shows that our model is accelerated expanding (see Table II) [46, 53, 54]. In Fig. 4c, the trajectories of ω pass via various stages of the evolution from very high redshift to low redshift. The EoS parameter explains as:

- (i) the model provides the ekpyrotic phase of the universe on the high redshift $z > 12.32$. In this model, the Big Bang is not the initial state of the Universe because the Big Bang is described as a collision of branes. Before the Big Bang, there is an ekpyrotic phase with the EoS $\omega \gg 1$,
- (ii) the Stiff-matter filled universe ($\omega = 1$),
- (iii) the Radiation phase ($\omega = \frac{1}{3}$),
- (iv) the hard universe ($\frac{1}{3} < \omega < 1$),
- (v) the dust-filled universe ($p = 0, \omega = 0$),
- (vi) the quintessence phase ($-1 < \omega < -\frac{1}{3}$).

Thus, we see that our model shows a quintessence model in the redshift range $0.05 \leq z \leq 3.27$ for all observational datasets OHD, *Pantheon*, and OHD+*Pantheon*.

A. The energy conditions

The energy conditions (ECs) play a significant role in describing the space-time singularity problems and analyzing the nature of null, space-like, time-like, or light-like geodesics in the classical GR. It provides an extensive range of grounds to study things like the conduct of cosmic geometries and the correlation that the stress-energy momentum (EMT) T_{ij} must comply positively. The energy conditions are just primitive constraints on different linear combinations of energy density ρ and pressure p . It shows that $\rho > 0$ and gravity are always attractive.

The preliminary ECs discussed in the literature inflict certain limitations on the stress tensor's capability to contract at each location in the space [55]. These ECs can also be drafted in a geometric and physical form that complies with

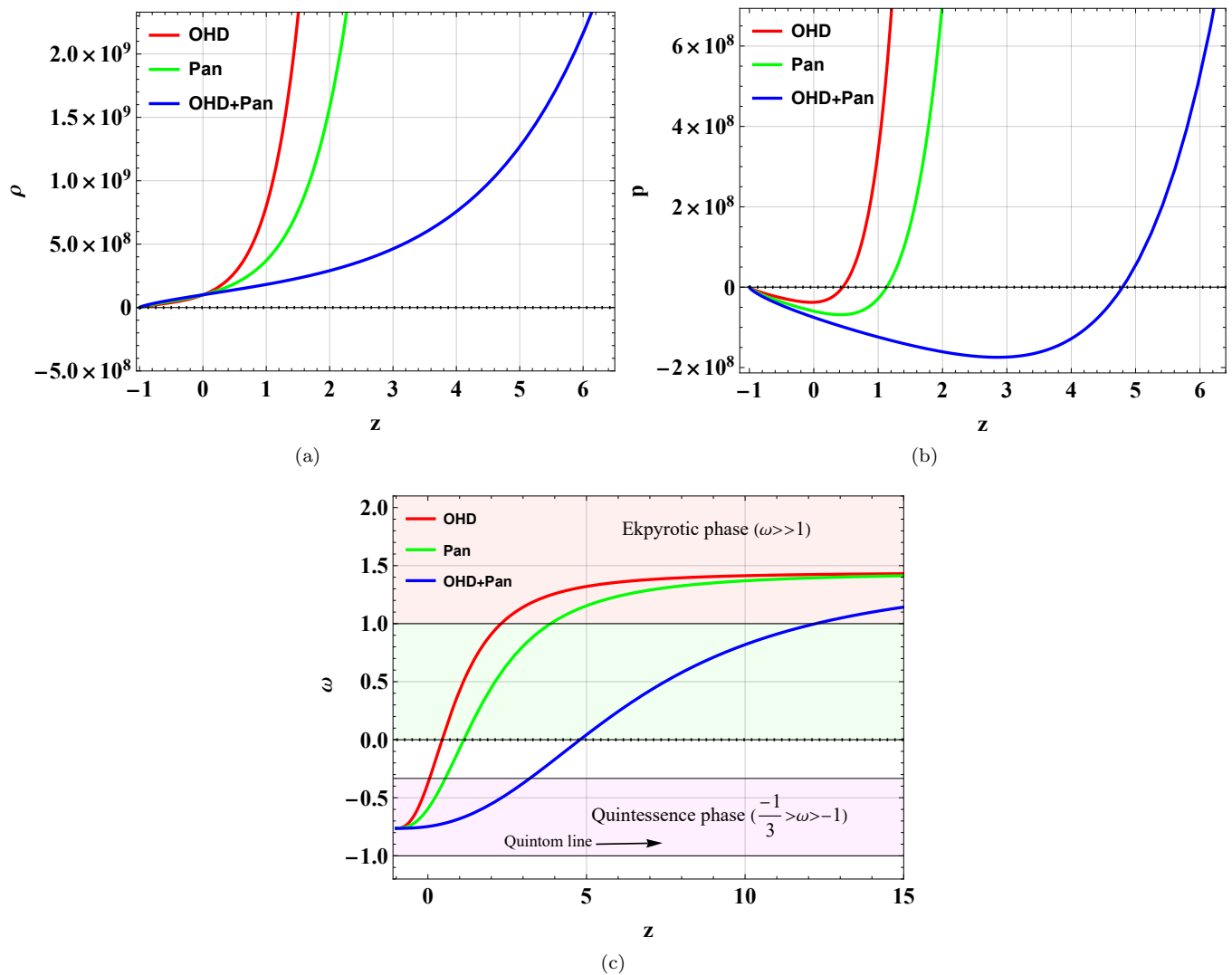


FIG. 4: The evolution of the ρ , p , and the EoS using $\zeta = -1.82$ and $\gamma = -0.9$.

Einstein's equation using R_{ij} and T_{ij} for a large number of theories. The ECs in various forms are discussed in Table III, where t^i and ξ^j are co-oriented time-like vectors and k^i is a null (light-like) vector. These ECs are dependent on each other [56].

The prior correlations are confined as:

- (i) Weak Energy Condition (WEC) \Rightarrow NEC;
- (ii) Strong Energy Condition (SEC) \Rightarrow NEC;
- (iii) Dominant Energy Condition (DEC) \Rightarrow NEC.

If the NEC is violated, then all the ECs are violated [57]. It is trusted, that the NEC is valid for all steady, well-behaved models of the Universe. A realistic model can violate other energy criteria by including an appropriate cosmological constant (either positive or negative). Wherever the T_{ij} violates the NEC, the model comes across destructive uncertainty like a ghost model in which the model has the *wrong* sign of the energy or exponentially expanding modes with informally short wavelengths which are referred to as *tachyons* [58]. The modified gravity theories can be envisaged as insignificant scalar backgrounds with a T_{ij} equal to a cosmological constant Λ . Consequently, they stand on the extremity of breaking the NEC. This describes how the degenerate dispersion relations came to be and it also indicates that these theories establish a first step in breaking the NEC.

The NEC plays a pivotal role among several ECs discussed in GR. In this condition, the EMT for matter T_{ij} satisfies $T_{ij}k^ik^j, \forall k^i$ i.e., for any vector satisfying $g_{ij}k^ik^j = 0$. Exceptionally, the following two bases for the NEC are interesting [59]:

TABLE III: Energy Conditions

Energy Condition	Physical conformation	Geometric conformation	Perfect conformation form
NEC	$T_{ij}k^ik^j \geq 0$	$R_{ij}k^ik^j \geq 0$	$\rho + p \geq 0$
WEC	$T_{ij}t^it^j \geq 0$	$G_{ij}t^it^j \geq 0$	$\rho \geq 0, \rho + p \geq 0$
SEC	$(T_{ij} - \frac{T}{n-2}g_{ij})t^it^j \geq 0$	$R_{ij}t^it^j \geq 0$	$\rho + p \geq 0, (n-3)\rho + (n-1)p \geq 0$
DEC	$T_{ij}t^i\xi^j \geq 0$	$G_{ij}t^i\xi^j \geq 0$	$\rho \geq p $

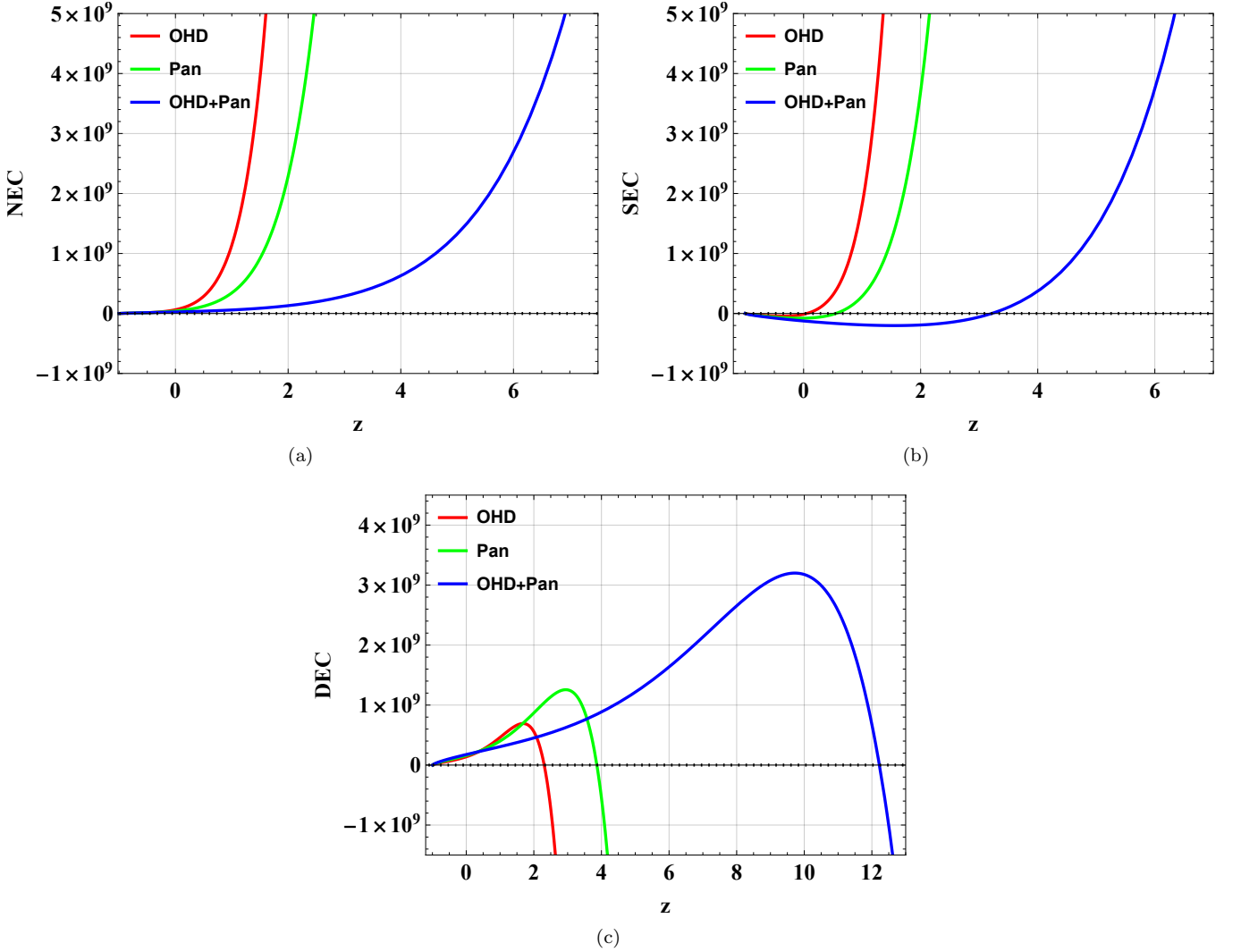


FIG. 5: The variations of the NEC, SEC, and DEC respectively.

- (1) Until rather recently the common mythology was that the NEC could not be violated in a healthy theory, except for scalar field non-minimally coupled to gravity [60].
- (2) The NEC is an important expectation of the Penrose singularity theorem [61], sustainable in GR. The theorem expects that (a) the NEC holds; (b) the Cauchy hypersurface is non-compact. The theorem reveals that the future will be singular once there is a trapped surface in space. A trapped surface is a closed surface on which outward-pointing light rays are converging.

The upper left panel of Fig. 5 shows that for all datasets, NEC is satisfied in this model. Whereas, Fig. 5b depicts that SEC violates our model, and violation of SEC indicates the presence of mysterious substances like dark energy and dark matter. Also, this is consistent with the recent observations. In contrast, the SEC is consistently violated across various best-fit values of the model parameters listed in Table II. This violation implies the universe's accelerated expansion in the distant future [34, 54, 64, 108–110].

In Fig. 5c, the plot of DEC shows that at early times DEC violates, though it satisfies at present and in late times.

B. The scalar field

Over the past few years, the quintessence model has convened great recognition in cosmology. This model is characterized by a quintessence-like scalar field because the EoS approaches in the range $-1 < \omega < -\frac{1}{3}$ which is consistent with recent observations in late times. According to the No-Go theorem, the EoS for a conventional scalar field model, described by a Lagrangian $L = L(\phi, \partial_\mu \phi \partial^\mu \phi)$, cannot pass over the Quintom line boundary ($\omega = -1$) [111, 112].

The model requisites an EoS close to $\omega \simeq -1$ to ensure good agreement with the recent observational datasets. This warrants that the kinetic energy (KE) of the scalar field, $\dot{\phi}^2$, be notably smaller than the potential energy (PE), $V(\phi)$, i.e., $\dot{\phi}^2 \ll V(\phi)$. When $\omega \simeq -1$, several models may be viewed to delineate the universe's acceleration, moreover, it can be redesigned for inflationary reasons. On this ground, our center of attention is on examining the models that utilize the scalar fields enclosed by the structure of $f(Q, T)$ -gravity. This approach enables us to analyze the possible improvement to the standard cosmology and comprehend the allusions of modified gravitational theories on the physical features of scalar fields and cosmic acceleration. The EoS ω converges to the redshift range $z \in (-1, -\frac{1}{3})$, hence this model is a quintessence model (see Fig. 4c).

The following action is defined in Einstein's theory of GR

$$S = \frac{c^4}{16\pi G} \int R \sqrt{-g} d^4x + L_m, \quad (30)$$

where L_m is indicated by L_{mq} , the action for the quintessence-like scalar field and taking $c = 1$ to normalize.

The action L_{mq} is given by

$$L_{mq} = \int \left(-\frac{1}{2} \partial_\mu \phi_q \partial^\mu \phi_q - V(\phi_q) \right) \sqrt{-g} d^4x. \quad (31)$$

In this condition, the scalar potential $V(\phi)$ assimilates to the self-interacting scalar field ϕ . Since ϕ is a function of t , therefore, it can be considered like a perfect fluid with energy density ρ_ϕ and pressure p_ϕ . Additionally, we can correlate these energy density ρ_{ϕ_q} and pressure p_{ϕ_q} of the quintessence-like scalar field in the scenario of FLRW cosmology as

$$\rho_{\phi_q} = \frac{1}{2} \dot{\phi}_q^2 + V(\phi_q), \quad p_{\phi_q} = \frac{1}{2} \dot{\phi}_q^2 - V(\phi_q). \quad (32)$$

The kinetic energy $\frac{1}{2} \dot{\phi}_q^2$ and the potential energy $V(\phi_q)$ are given by

$$\frac{1}{2} \dot{\phi}_q^2 = - \frac{24H_0^4 (1+z)^{4(1-\sqrt{2/3})} \left(e^{2\sqrt{6}\alpha} + (1+z)^{\sqrt{6}} \right)^{5/3} \left((-3+\sqrt{6}) e^{2\sqrt{6}\alpha} + (3+\sqrt{6})(1+z)^{\sqrt{6}} \right) \zeta}{\left(1 + e^{2\sqrt{6}\alpha} \right)^{8/3} (8\pi + \gamma)}, \quad (33)$$

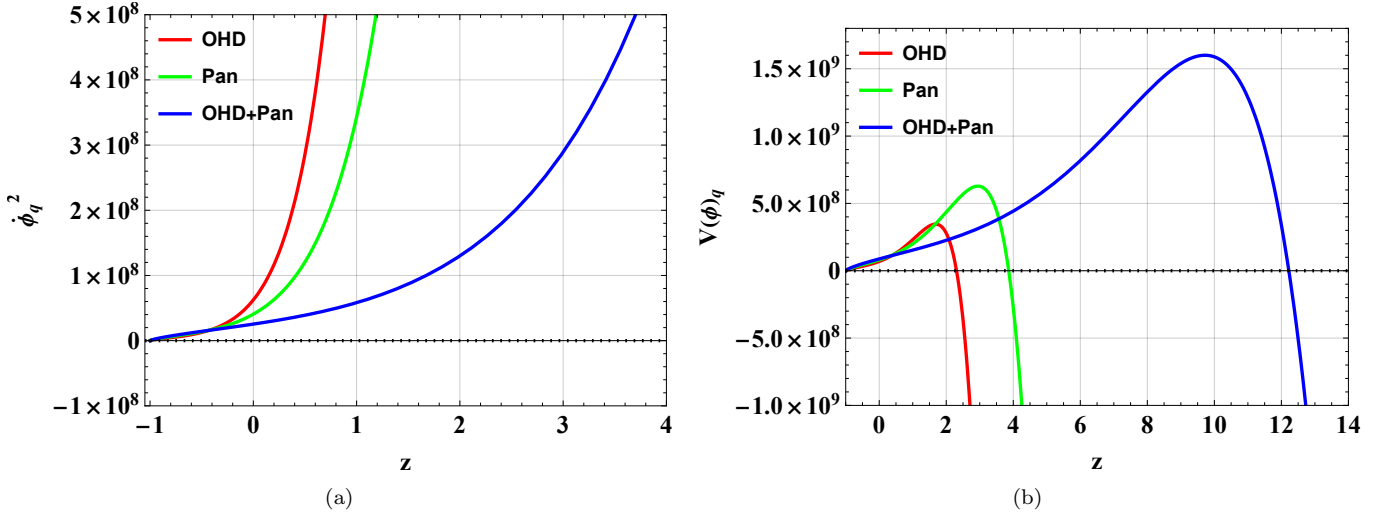


FIG. 6: The evolution of the $\dot{\phi}_q^2$ and the $V(\phi_q)$.

$$V(\phi_q) = -\frac{3H_0^4 (1+z)^{4(1-\sqrt{2/3})} \left(e^{2\sqrt{6}\alpha} + (1+z)^{\sqrt{6}}\right)^{5/3} \left((3+2\sqrt{6})e^{2\sqrt{6}\alpha} + (3-2\sqrt{6})(1+z)^{\sqrt{6}}\right) \zeta}{\left(1+e^{2\sqrt{6}\alpha}\right)^{8/3} (4\pi + \gamma)}. \quad (34)$$

In Fig. 6, the trajectories describe the evolution of the kinetic term $\frac{1}{2}\dot{\phi}_q^2$ and the potential term $V(\phi_q)$ of the energy for the quintessence-like scalar field in terms of the redshift z in the $f(Q, T)$ theory of gravity. At the early evolution, the kinetic energy of the quintessence-like field is infinitely large and as time elapses, these values decrease monotonically, approaching zero as $z \rightarrow -1$ asymptotically.

Initially, the potential energy $V(\phi_q)$ is incapacitated in the redshift range $2.36 > z > 12.29$ for all observations, over time decrease monotonically, and tending to zero as $z \rightarrow -1$ asymptotically in the redshift range less than $z < 2.36$ (OHD). Thus, we see that the $\dot{\phi}_q^2$ declines more rapidly than $V(\phi_q)$. The kinetic and potential energies of the quintessence-like field show similar minimizing nature over time.

C. The slow-roll parameters

The slow-roll parameter is a fundamental criterion describing the inflationary dynamics and they have been extensively studied in various cosmological contexts. This parameter can be stated either in terms of the inflaton potential or the Hubble parameter H , allowing for the analysis of both standard and non-standard cosmologies including the braneworld scenarios [113]. The slow-roll parameter closely resembles the cosmography parameters, which are used to constrain inflationary models and express key inflationary quantities like the spectral index and tensor-to-scalar ratio [114].

The following constraints must be fulfilled to occur in a new inflationary scenario:

1. The inflaton rolls slowly down the potential, meaning the velocity of the field $\dot{\phi}$ is small, being ϕ the scalar field corresponding to the potential $V(\phi)$.
2. The curvature of the potential $V(\phi)$ is sufficiently flat as compared to the large vacuum energy so that $\ddot{\phi}$ is small.
3. The inflaton particles must have little mass.

These conditions are quantified using the slow-roll parameters, the dimensionless quantities that measure how slowly the inflaton field evolves.

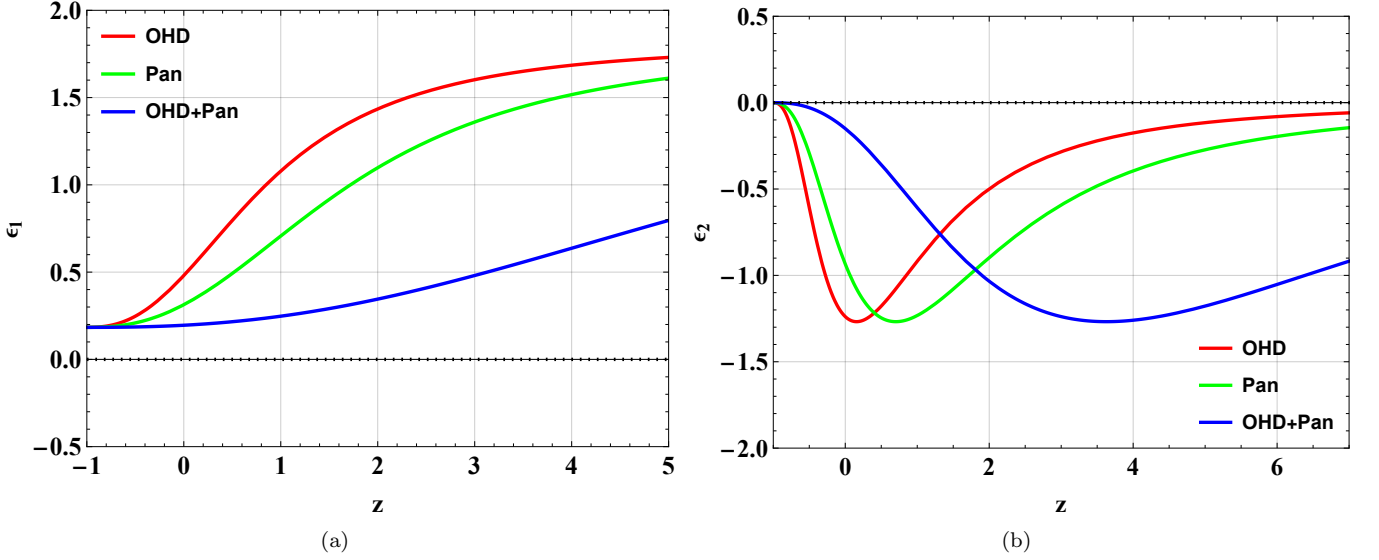


FIG. 7: The evolution of the ϵ_1 and ϵ_2 .

The first and the second kind of slow-roll parameters denoted by ϵ_1 , and ϵ_2 are defined as [115, 116]:

$$\epsilon_1(t) = -\frac{\dot{H}}{H^2}. \quad (35)$$

and

$$\epsilon_2(t) = \frac{\ddot{H}}{\dot{H}H} - \frac{2\dot{H}}{H^2}. \quad (36)$$

Using the equations,

$$\dot{H} = -(1+z)H(z)\frac{dH}{dz} \quad (37)$$

and

$$\ddot{H} = (1+z)^2 (H(z))^2 \frac{d^2H}{dz^2} + 2(H(z))^2 (1+z) \frac{dH}{dz} + (1+z)^2 H(z) \left(\frac{dH}{dz}\right)^2 - (1+z)(H(z))^2 \frac{dH}{dz}, \quad (38)$$

and H from Eq. (22) in Eqs. (35) and (36), we obtain the values of both slow-roll parameters in terms of z . The graphs are depicted in Fig. 7 with the help of these obtained values.

The first slow-roll parameter ϵ_1 quantifies how flat the potential $V(\phi)$ is, i.e., this parameter measures the steepness of the potential, and the second slow-roll parameter ϵ_2 measures the curvature of the potential. The condition for inflation regarding the first slow-roll parameter ϵ_1 can be taken as $\epsilon_1 \ll 1$, and the inflation will continue as long as the second slow-roll parameter ϵ_2 satisfies $|\epsilon_2| \ll 1$.

Figs. 7a depict that the first slow-roll parameter satisfies the condition $\epsilon_1 \ll 1$ as $z \rightarrow -1$, and the second slow-roll parameter obeys the condition $|\epsilon_2| \ll 1$ as $z \rightarrow -1$ for all the observational datasets. Thus, it can be said that the slow-roll inflation sustained for those values of z at which both the conditions $\epsilon_1 \ll 1$ and $|\epsilon_2| \ll 1$ because $\lim_{z \rightarrow -1} \epsilon_1, |\epsilon_2| = 0$. These conditions imply that the inflaton field rolls slowly enough so that the universe undergoes sufficient inflation and solves the horizon problem and flatness problem.

V. THE CONCLUDING REMARKS

In this work, we have explored an expansion of the third identical characterization of GR known as the symmetric teleparallel formulation. This expansion is known as the $f(Q, T)$ theory of gravity. Its theory involves a

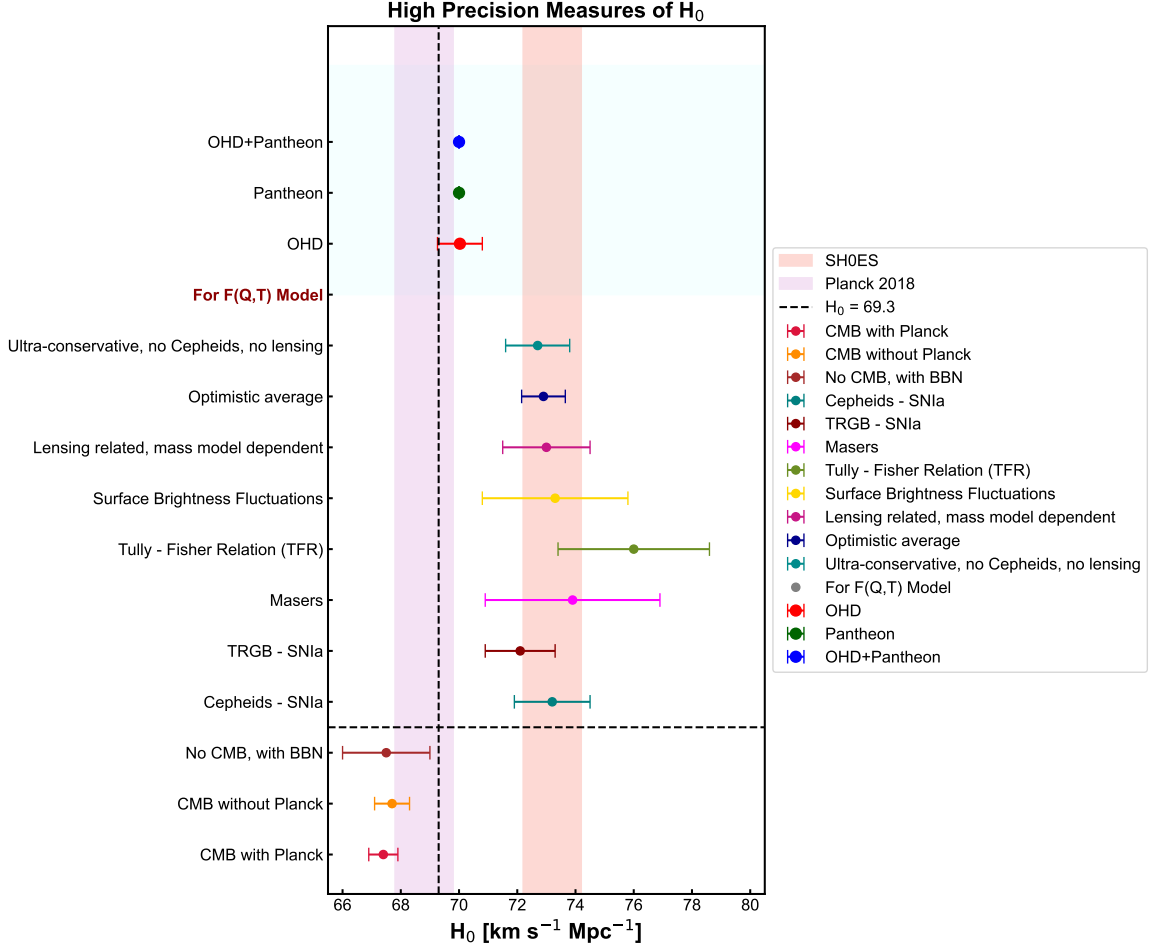


FIG. 8: The recent approximations of the H_0 -tension evaluated from the OHD, Pantheon, and OHD+Pantheon datasets respectively.

non-minimal coupling between Q and T of the EMT expressed as $f(Q, T) = f_1(Q) + f_2(T)$, a configuration extensively studied in the existing literature. In our analysis, we specified $f_1(Q) = \zeta Q^2$ with $\zeta < 0$ and $f_2(T) = \gamma T$. We consider the jerk parameter $j = \exp(q)$ to avoid the calculation's complications and proceed to find the appropriate solutions for several physical parameters. We use the MCMC method by executing the *emcee codes* in Python using various observational datasets explained in Figs. 1. In many significant examinations, we found the two-dimensional posterior classifications of the parameters H_0 , and α at 1σ and 2σ confidence levels (CLs) imparting constraints on these.

The error bar trajectories of $H(z)$, and $\mu(z)$ concerning redshifts z reveal the extent of the compatibility between the obtained model and the Λ CDM. These plots indicate the deflections of our model from the Λ CDM at the early evolution. Both later coincide with Λ CDM in divergent observational datasets (see Figs. 2). The recent approximations of the H_0 -tension obtained from the OHD, Pantheon, and OHD+Pantheon datasets respectively can be seen in Fig. 8.

The current value of the parameters H , q , and α for distinct observations are shown in Table II. We have discussed the nature of the q for good-fit values in Fig. 3a, where q transits from deceleration to acceleration in the redshift range $0.85 \geq z_{tr} \leq 6.39$. Thus, the model is accelerating at present. The jerk parameter j is positive for every redshift range and tends to 0.5 in late times, as shown in Fig. 3b. The evolution of ρ is always positive and decreases monotonically as the cosmic redshift z decreases over time (see Fig. 4a).

The isotropic pressure p transits from positive to negative in the interval of the redshift $0.47 > z < 4.79$, and shows the dust-filled Universe at $z \approx 0.47, 1.14, 4.79$ for the observations OHD, Pantheon, and OHD+Pantheon respectively. This shows the negative conduct for every constraint in late times and converges to zero at $z \rightarrow -1$. The model demonstrates the existence of dark energy that enforces the accelerating expansion at later times (see Fig. 4b). The EoS traverses from positive to negative which tends to -1 as shown in Fig. 4c. The model begins with the Ekpyrotic phase ($\omega \gg 1$), Perfect fluid phase ($0 \geq \omega \geq 1$), and Quintessence phase ($-\frac{1}{3} > \omega > -1$). Hence, the

model conducts like the quintessence model at later times.

In Fig. 5, It has been seen that the model fulfills all the criteria of ECs except SEC in the later times which suggests the presence of dark energy at later times. In this model, the DEC is disobeyed for the higher redshift which validates the Ekpyrotic phase of the Universe, and it is satisfied belated. Specifically, the clear tendency of DEC accomplishment at low redshift is similar to what was found by Lima et al. [117, 118]. The belated defiance of SEC is directly correlated with the current accelerated expanding nature of the universe [53].

The evolutions of the quintessence-like KE and PE decrease monotonically concerning the redshift z , tending to zero as $z \rightarrow -1$, and the quintessence-like KE decreases more rapidly than the quintessence-like PE at low redshift for all observations. The quintessence-like potential energy is violated at high redshift $z > 2$ (see Fig. 6). Figs. 7 demonstrate that the slow-roll inflation sustained for those values of z at which both the conditions $\epsilon_1 \ll 1$ and $|\epsilon_2| \ll 1$. These conditions imply that the inflaton field rolls slowly enough so that the universe undergoes sufficient inflation and solves the horizon and the flatness problems.

Finally, our study exhibits that the quintessence model in $f(Q, T)$ -gravity imparts viable support for comprehension of the universe's evolution. It effectively assimilates the requisite for observational data and provides an understanding of the energy conditions and steadiness of the universe. The review of the model endows wide-ranging interpretations of cosmology and the plausible performance of modified gravity theories elaborating on the universe's accelerated expanding nature and comprehensive dynamics. The upcoming projects will speculate further investigations into the suggestions of these consequences and the prospective for observational accreditation.

ACKNOWLEDGEMENT

The authors J. K. Singh and Shaily thank the Department of Mathematics, NSUT, New Delhi-78, India, and Bennett University, Greater Noida, India for providing the necessary facilities where a part of this work has been completed.

DATA AVAILABILITY STATEMENT

In this manuscript, we have used observational data as available in the literature as such our work does not produce any form of new data.

-
- [1] G. Hinshaw *et al.* [WMAP], *Astrophys. J. Suppl.* **208**, 19 (2013).
 - [2] M. Tegmark *et al.* [SDSS], *Phys. Rev. D* **69**, 103501 (2004).
 - [3] U. Seljak *et al.* [SDSS], *Phys. Rev. D* **71**, 103515 (2005).
 - [4] L. Anderson *et al.* [BOSS], *Mon. Not. Roy. Astron. Soc.* **427**, no.4, 3435-3467 (2013).
 - [5] D. J. Eisenstein *et al.* [SDSS], *Astrophys. J.* **633**, 560-574 (2005).
 - [6] B. Jain and A. Taylor, *Phys. Rev. Lett.* **91**, 141302 (2003).
 - [7] N. Aghanim *et al.* [Planck], *Astron. Astrophys.* **641**, A6 (2020) [erratum: *Astron. Astrophys.* **652**, C4 (2021)].
 - [8] M. Carmeli, E. Leibowitz and N. Nissani, "Gravitation: $SL(2, C)$ gauge theory and conservation laws," World Scientific, Chapter 4, Singapore (1990).
 - [9] A. Einstein, "The meaning of Relativity, Fifth Edition," Princeton University Press **129** (1956).
 - [10] H. Yilmaz, *Nuovo Cimento B* **107**, 941-960 (1992).
 - [11] A. S. Eddington, "The Mathematical Theory of Relativity," Cambridge University Press, (1923).
 - [12] R. V. Wagoner, *Phys. Rev. D* **1**, 3209-3216 (1970).
 - [13] S. S. Yazadjiev, D. D. Doneva and D. Popchev, *Phys. Rev. D* **93**, no.8, 084038 (2016).
 - [14] I. Quiros, *Int. J. Mod. Phys. D* **28**, no.07, 1930012 (2019).
 - [15] J. K. Singh, *Mod. Phys. Lett. A* **25** (2010), 2363-2371.
 - [16] J. K. Singh, *Int. J. Theor. Phys.* **48** (2009), 905-912.
 - [17] J. K. Singh, *Astrophys. Space Sci.* **281** (2002), 585-594.
 - [18] J. K. Singh and N. K. Sharma, *Int. J. Theor. Phys.* **49** (2010), 2902-2909.
 - [19] C. Brans and R. H. Dicke, *Phys. Rev.* **124**, 925-935 (1961).
 - [20] J. Solà Peracaula, A. Gomez-Valent, J. de Cruz Pérez and C. Moreno-Pulido, *Astrophys. J. Lett.* **886**, no.1, L6 (2019).
 - [21] J. K. Singh, N. K. Sharma and A. Beesham, *Theor. Math. Phys.* **193** (2017) no.3, 1865-1879.
 - [22] A. H. Ziaie, H. Shabani and H. Moradpour, *Eur. Phys. J. Plus* **139**, no.2, 148 (2024).
 - [23] S. Nojiri, S. D. Odintsov and V. K. Oikonomou, *Phys. Rept.* **692**, 1-104 (2017).

- [24] S. I. dos Santos, G. A. Carvalho, P. H. R. S. Moraes, C. H. Lenzi and M. Malheiro, *Eur. Phys. J. Plus* **134**, no.8, 398 (2019).
- [25] E. Elizalde and M. Khurshudyan, *Phys. Rev. D* **99**, no.2, 024051 (2019).
- [26] J. K. Singh, H. Balhara, Shaily and P. Singh, *Astron. Comput.* **46**, 100795 (2024).
- [27] J. K. Singh, Shaily, A. Singh, A. Beesham and H. Shabani, *Annals Phys.* **455**, 169382 (2023).
- [28] M. Sharif and A. Siddiqa, *Gen. Rel. Grav.* **51**, no.6, 74 (2019).
- [29] S. Bhattacharjee and P. K. Sahoo, *Phys. Dark Univ.* **28**, 100537 (2020).
- [30] J. K. Singh, H. Balhara, K. Bamba and J. Jena, *JHEP* **03**, 191 (2023) [erratum: *JHEP* **04**, 049 (2023)].
- [31] J. K. Singh, A. Singh, G. K. Goswami and J. Jena, *Annals Phys.* **443**, 168958 (2022).
- [32] R. Nagpal, S. K. J. Pacif, J. K. Singh, K. Bamba and A. Beesham, *Eur. Phys. J. C* **78**, no.11, 946 (2018).
- [33] J. K. Singh, K. Bamba, R. Nagpal and S. K. J. Pacif, *Phys. Rev. D* **97**, no.12, 123536 (2018).
- [34] J. K. Singh, Shaily, H. Balhara, S. G. Ghosh and S. D. Maharaj, *Phys. Dark Univ.* **45** (2024), 101513.
- [35] Shaily, A. Singh, J. K. Singh and S. Ray, *Astron. Comput.* **49** (2024), 100876.
- [36] Shaily, J. K. Singh and A. Singh, *Fortsch. Phys.*, (2024).
- [37] J. K. Singh, Shaily, H. Balhara, K. Bamba and J. Jena, *Astron. Comput.* **46**, 100790 (2024).
- [38] J. K. Singh, Shaily and K. Bamba, *Chin. J. Phys.* **84**, 371-380 (2023).
- [39] R. Rani, Shaily, G. K. Goswami and J. K. Singh, *JHEAp* **45** (2025), 168-180.
- [40] J. K. Singh, Shaily, R. Myrzakulov and H. Balhara, *New Astron.* **104**, 102070 (2023).
- [41] J. K. Singh, Shaily, A. Singh, H. Balhara and J. R. L. Santos, *Annals Phys.* **469** (2024), 169781.
- [42] Shaily, J. K. Singh, M. Tyagi and J. R. L. Santos, [arXiv:2411.00032 [gr-qc]].
- [43] T. Harko and F. S. N. Lobo, Cambridge University Press, 2018, ISBN 978-1-108-42874-3, 978-1-108-58457-9.
- [44] J. K. Singh, H. Balhara, Shaily, T. Q. Do and J. Jena, *Astron. Comput.* **47**, 100800 (2024).
- [45] Shaily, J. K. Singh, J. R. L. Santos and M. Zeyauddin, *Int. J. Mod. Phys. D*, (2024).
- [46] J. K. Singh, Shaily, S. Ram, J. R. L. Santos and J. A. S. Fortunato, *Int. J. Mod. Phys. D* **32**, no.07, 2350040 (2023).
- [47] A. Golovnev and M. J. Guzmán, *Int. J. Geom. Meth. Mod. Phys.* **18**, no.supp01, 2140007 (2021).
- [48] Y. F. Cai, S. Capozziello, M. De Laurentis and E. N. Saridakis, *Rept. Prog. Phys.* **79**, no.10, 106901 (2016).
- [49] H. Balhara, J. K. Singh, Shaily and E. N. Saridakis, *Symmetry* **16** (2024), 1299.
- [50] J. K. Singh, A. Singh, Shaily and J. Jena, *Chin. J. Phys.* **86**, 616-627 (2023).
- [51] G. Kofinas and E. N. Saridakis, *Phys. Rev. D* **90**, 084045 (2014).
- [52] M. M. Gohain and K. Bhuyan, *Phys. Dark Univ.* **43**, 101424 (2024).
- [53] J. K. Singh, A. Singh, Shaily, S. G. Ghosh and S. D. Maharaj, *Phys. Scr.* **99**, 125001 (2024).
- [54] J. K. Singh, Shaily, A. Pradhan and A. Beesham, *Phys. Dark Univ.* **46** (2024), 101658.
- [55] E. Curiel, *Einstein Stud.* **13**, 43-104 (2017).
- [56] E. A. Kontou and K. Sanders, *Class. Quant. Grav.* **37** (2020) no.19, 193001.
- [57] M. Visser, "Lorentzian wormholes: From Einstein to Hawking,"
- [58] R. R. Caldwell, *Phys. Lett. B* **545**, 23-29 (2002)
- [59] V. A. Rubakov, *Phys. Usp.* **57** (2014), 128-142.
- [60] E. E. Flanagan and R. M. Wald, *Phys. Rev. D* **54** (1996), 6233-6283.
- [61] R. Penrose, *Phys. Rev. Lett.* **14** (1965), 57-59.
- [62] Shaily, A. Singh, J. K. Singh, S. Hussain and R. Myrzakulov, [arXiv:2402.08709 [gr-qc]].
- [63] G. K. Goswami, R. Rani, H. Balhara and J. K. Singh, *Indian J. Phys.* **97**, no.12, 3707-3714 (2023).
- [64] J. K. Singh and R. Nagpal, *Eur. Phys. J. C* **80**, no.4, 295 (2020).
- [65] J. L. Lehners, *Phys. Rept.* **465** (2008), 223-263.
- [66] M. Koussour and M. Bennai, *Chin. J. Phys.* **79**, 339-347 (2022).
- [67] M. Koussour, S. H. Shekh and M. Bennai, *JHEAp* **35**, 43-51 (2022).
- [68] M. Koussour, S. H. Shekh and M. Bennai, *Phys. Dark Univ.* **36**, 101051 (2022).
- [69] M. Koussour, K. El Bourakadi, S. H. Shekh, S. K. J. Pacif and M. Bennai, *Annals Phys.* **445**, 169092 (2022).
- [70] S. A. Narawade, L. Pati, B. Mishra and S. K. Tripathy, *Phys. Dark Univ.* **36**, 101020 (2022).
- [71] G. K. Goswami, R. Rani, J. K. Singh and A. Pradhan, *JHEAp* **43** (2024), 105-113.
- [72] F. Bajardi, D. Vernieri and S. Capozziello, *Eur. Phys. J. Plus* **135**, no.11, 912 (2020).
- [73] K. Hu, T. Paul and T. Qiu, *Sci. China Phys. Mech. Astron.* **67**, no.2, 220413 (2024).
- [74] T. Harko, T. S. Koivisto, F. S. N. Lobo, G. J. Olmo and D. Rubiera-Garcia, *Phys. Rev. D* **98**, no.8, 084043 (2018).
- [75] S. Capozziello, M. Capriolo and S. Nojiri, *Phys. Lett. B* **850**, 138510 (2024).
- [76] K. Hu, M. Yamakoshi, T. Katsuragawa, S. Nojiri and T. Qiu, *Phys. Rev. D* **108**, no.12, 124030 (2023).
- [77] L. Heisenberg, *Phys. Rept.* **1066**, 1-78 (2024).
- [78] S. Arora, J. R. L. Santos and P. K. Sahoo, *Phys. Dark Univ.* **31**, 100790 (2021).
- [79] N. Myrzakulov, M. Koussour, A. H. A. Alfedeel and H. M. Elkhair, *Chin. J. Phys.* **86**, 300-312 (2023).
- [80] S. Arora, A. Parida and P. K. Sahoo, *Eur. Phys. J. C* **81**, no.6, 555 (2021).
- [81] A. P. Kale, Y. S. Solanke, S. H. Shekh and A. Pradhan, *Symmetry* **15**, no.10, 1835 (2023).
- [82] J. A. Nájera and C. A. Alvarado, *Phys. Dark Univ.* **38**, 101141 (2022).
- [83] J. Z. Yang, S. Shahidi, T. Harko and S. D. Liang, *Eur. Phys. J. C* **81**, no.2, 111 (2021).
- [84] G. Gadbail, S. Arora and P. K. Sahoo, *Eur. Phys. J. Plus* **136**, no.10, 1040 (2021).
- [85] G. N. Gadbail, S. Arora and P. K. Sahoo, *Eur. Phys. J. C* **81**, no.12, 1088 (2021).
- [86] Y. Xu, G. Li, T. Harko and S. D. Liang, *Eur. Phys. J. C* **79**, no.8, 708 (2019).

- [87] S. Arora, S. K. J. Pacif, S. Bhattacharjee and P. K. Sahoo, *Phys. Dark Univ.* **30** (2020), 100664.
- [88] S. Arora and P. K. Sahoo, *Phys. Scripta* **95**, no.9, 095003 (2020).
- [89] N. Godani and G. C. Samanta, *Int. J. Geom. Meth. Mod. Phys.* **18**, no.09, 2150134 (2021).
- [90] A. Nájera and A. Fajardo, *JCAP* **03**, no.03, 020 (2022).
- [91] Y. Xu, T. Harko, S. Shahidi and S. D. Liang, *Eur. Phys. J. C* **80**, no.5, 449 (2020).
- [92] D. Rapetti, S. W. Allen, M. A. Amin and R. D. Blandford, *Mon. Not. Roy. Astron. Soc.* **375**, 1510-1520 (2007).
- [93] Z. X. Zhai, M. J. Zhang, Z. S. Zhang, X. M. Liu and T. J. Zhang, *Phys. Lett. B* **727**, 8-20 (2013).
- [94] K. Asvesta, L. Kazantzidis, L. Perivolaropoulos and C. G. Tsagas, *Mon. Not. Roy. Astron. Soc.* **513**, no.2, 2394-2406 (2022).
- [95] A. G. Riess, R. P. Kirshner, B. P. Schmidt, S. Jha, P. Challis, P. M. Garnavich, A. A. Esin, C. Carpenter, R. Grashius and R. E. Schild, *et al. Astron. J.* **117**, 707-724 (1999).
- [96] S. Jha, R. P. Kirshner, P. Challis, P. M. Garnavich, T. Matheson, A. M. Soderberg, G. J. M. Graves, M. Hicken, J. F. Alves and H. G. Arce, *et al. Astron. J.* **131**, 527-554 (2006).
- [97] M. Hicken, P. Challis, S. Jha, R. P. Kirshner, T. Matheson, M. Modjaz, A. Rest and W. M. Wood-Vasey, *Astrophys. J.* **700**, 331-357 (2009).
- [98] M. Hicken, W. M. Wood-Vasey, S. Blondin, P. Challis, S. Jha, P. L. Kelly, A. Rest and R. P. Kirshner, *Astrophys. J.* **700**, 1097-1140 (2009).
- [99] M. Hicken, P. Challis, R. P. Kirshner, A. Rest, C. E. Cramer, W. M. Wood-Vasey, G. Bakos, P. Berlind, W. R. Brown and N. Caldwell, *et al. Astrophys. J. Suppl.* **200**, 12 (2012).
- [100] C. Contreras, M. Hamuy, M. M. Phillips, G. Folatelli, N. B. Suntzeff, S. E. Persson, M. Stritzinger, L. Boldt, S. Gonzalez and W. Krzeminski, *et al. Astron. J.* **139**, 519-539 (2010).
- [101] M. Sako *et al.* [SDSS], *Publ. Astron. Soc. Pac.* **130**, no.988, 064002 (2018).
- [102] J. Guy *et al.* [SNLS], *Astron. Astrophys.* **523**, A7 (2010).
- [103] D. M. Scolnic *et al.* [Pan-STARRS1], *Astrophys. J.* **859**, no.2, 101 (2018).
- [104] N. Suzuki *et al.* [Supernova Cosmology Project], *Astrophys. J.* **746**, 85 (2012).
- [105] A. G. Riess, S. A. Rodney, D. M. Scolnic, D. L. Shafer, L. G. Strolger, H. C. Ferguson, M. Postman, O. Graur, D. Maoz and S. W. Jha, *et al. Astrophys. J.* **853**, no.2, 126 (2018).
- [106] A. G. Riess *et al.* [Supernova Search Team], *Astrophys. J.* **607**, 665-687 (2004).
- [107] A. G. Riess, L. G. Strolger, S. Casertano, H. C. Ferguson, B. Mobasher, B. Gold, P. J. Challis, A. V. Filippenko, S. Jha and W. Li, *et al. Astrophys. J.* **659**, 98-121 (2007).
- [108] Y. L. Bolotin, V. A. Cherkaskiy, O. A. Lemets, D. A. Yerokhin and L. G. Zazunov, [arXiv:1502.00811 [gr-qc]].
- [109] M. Visser, *Science* **276** (1997), 88-90.
- [110] M. Visser, *Phys. Rev. D* **56** (1997), 7578-7587.
- [111] J. Q. Xia, Y. F. Cai, T. T. Qiu, G. B. Zhao and X. Zhang, *Int. J. Mod. Phys. D* **17** (2008), 1229-1243.
- [112] Y. F. Cai, T. Qiu, Y. S. Piao, M. Li and X. Zhang, *JHEP* **10** (2007), 071.
- [113] G. Calcagni, *Phys. Rev. D* **69**, 103508 (2004).
- [114] D. Das, S. Dutta and S. Chakraborty, *Mod. Phys. Lett. A* **33**, no.26, 1850151 (2018).
- [115] M. Shiravand, S. Fakhry and M. Farhoudi, *Phys. Dark Univ.* **37**, 101106 (2022).
- [116] A. R. Liddle, P. Parsons and J. D. Barrow, *Phys. Rev. D* **50** (1994), 7222-7232.
- [117] M. P. Lima, S. Vitenti and M. J. Reboucas, *Phys. Rev. D* **77** (2008), 083518.
- [118] M. P. Lima, S. D. P. Vitenti and M. J. Reboucas, *Phys. Lett. B* **668** (2008), 83-86.